Phase-field simulation of two-phase micro-flows in a Hele-Shaw cell

Y. Sun & C. Beckermann
Department of Mechanical and Industrial Engineering, University of Iowa, USA

Abstract

A two-phase diffuse interface model previously developed by the authors is used to simulate the buoyancy-driven flow and Rayleigh-Taylor instability of fluid layers inside a Hele-Shaw cell. The model assumes that the two phases coexist inside the diffuse interface with different properties and velocities. A separate momentum equation is used to calculate the slip velocity between the two phases within the diffuse interface. This two-phase approach is coupled with a phase-field equation for calculating the interface motion. The model is validated by comparing the calculated interface evolution, before any topology changes occur, to available results from a sharp interface model. Then, the flows and interface topology changes are investigated for fluid layers with a large density and viscosity contrasts. The convergence of the results with respect to the interface width is examined in detail. It is shown that the two-phase model converges better than standard diffuse interface models that assume a single velocity inside the diffuse interface.

1 Introduction

Two-phase flows featuring topology transitions and other interface singularities have become an area of increasing research interest over the last decade [1-3]. In such flows, multiple length and time scales emerge and capillary stresses cannot be neglected. For the nano-scale phenomena introduced by interface singularities, conventional sharp interface models fail to work. Diffuse interface approaches have been proposed to overcome these difficulties [1, 4, 5]. In diffuse interface models, the interface is viewed as a region of finite extent over which the properties vary smoothly from one phase to the other.

WIT Transactions on Engineering Sciences, Vol 50, © 2005 WIT Press
www.witpress.com, ISSN 1743-3533 (on-line)

All thermodynamically derived diffuse interface models [1, 2, 4] assume the existence of a single velocity and pressure at any point inside the diffuse interface between two phases. Moreover, single thermophysical properties (e.g., density and viscosity) are assumed to exist and their variation across the diffuse interface is postulated in some *ad-hoc* manner. For large differences in these properties between the phases, such diffuse interface models can give results that are very dependent on the choice of the interface width [6] and the way the property variations are specified [7]. Based on an atomic-scale ensemble averaging approach, a so-called "two-phase" diffuse interface model was recently developed by the present authors [6]. As opposed to thermodynamically derived diffuse interface models, the two phases are assumed to coexist inside the diffuse interface with different properties, velocities, and pressures. The phase interactions are modelled explicitly through the inclusion of interfacial forces in the momentum equations for each phase. Capillary stresses inside the diffuse interface are included in the model as well. One unique feature of the model is that the results are independent of the diffuse interface width for simple shear flows. This allows for artificially large interface widths and hence significantly improves computational efficiency.

In the present study, the two-phase diffuse interface model from [6] is applied to a buoyancy-driven flow inside a Hele-Shaw cell that features interface topology transitions. The motion of the interface between the two phases is calculated using a phase-field equation [8]. The two-phase model is compared to a mixture model that assumes a zero slip velocity inside the diffuse interface and is equivalent to thermodynamically derived models. The objective of this paper is to examine the differences in the predictions between the two-phase and mixture diffuse interface models for large density and viscosity contrasts between the phases. The convergence of the results from the two models with respect to the interface width is compared in detail.

2 Model equations

2.1 Two-phase model

The present study considers the flow of two viscous fluids of different properties (i.e., density and viscosity) inside a Hele-Shaw cell. The cell has a gap of width b that is much smaller than the cell length L (i.e., $b << L$), as illustrated in Fig. 1. The two-phase diffuse interface model of Sun and Beckermann [6] is simplified in the following using the standard Hele-Shaw approximations [9].

2.1.1 Continuity

In the absence of phase change, the two-phase continuity equations are given by

$$\nabla \cdot \boldsymbol{u} = (\rho_1 - \rho_2)\nabla \cdot \left[\frac{\phi(1-\phi)}{\rho} \Delta \boldsymbol{u} \right] \tag{1}$$

$$\frac{\partial \phi}{\partial t} + \boldsymbol{u} \cdot \nabla \phi + \rho \nabla \cdot \left(\frac{\phi(1-\phi)}{\rho} \Delta \boldsymbol{u} \right) = 0 \tag{2}$$

where ρ_1 and ρ_2 are the densities of phases 1 and 2, respectively, $\rho = \rho_1\phi + \rho_2(1-\phi)$ is the mixture density, $\boldsymbol{u} = \left[\rho_1\phi\boldsymbol{u}_1 + \rho_2(1-\phi)\boldsymbol{u}_2\right]/\rho$ is the mixture velocity averaged across the gap width b, $\boldsymbol{u}_1$ and $\boldsymbol{u}_2$ are the gap averaged velocities of the two phases, and ϕ is the phase field. The phase field varies in a hyperbolic tangent fashion across the diffuse interface, as illustrated in Fig. 2, and takes on constant values of $\phi = 1$ and $\phi = 0$ inside phases 1 and 2, respectively. It can be viewed as an atomic-scale volume fraction [5]. The parameter δ in Fig. 2 is a measure of the interface width, with ϕ varying from 0.95 to 0.05 within 6δ. The concept of a slip velocity, $\Delta\boldsymbol{u} = \boldsymbol{u}_1 - \boldsymbol{u}_2$, inside the diffuse interface is illustrated in Fig. 3. In the so-called mixture model, $\Delta\boldsymbol{u}$ is equal to zero.

Note that the right-hand side of Eq. (1) is generally non-zero for $\rho_1 \neq \rho_2$. Hence, the present two-phase approach introduces compressibility inside the diffuse interface, even though the individual phases are incompressible. Equation (2) is the evolution equation for the phase-field, ϕ. This advection equation also contains an extra term due to the slip velocity [6]. To solve it numerically, Eq. (2) is rewritten as

$$\frac{\partial\phi}{\partial t} + \boldsymbol{u}\cdot\nabla\phi + \rho\nabla\cdot\left(\frac{\phi(1-\phi)}{\rho}\Delta\boldsymbol{u}\right) = M\left[\nabla^2\phi - \frac{\phi(1-\phi)(1-2\phi)}{\delta^2} - |\nabla\phi|\nabla\cdot\left(\frac{\nabla\phi}{|\nabla\phi|}\right)\right] \quad (3)$$

where M is a purely numerical parameter. The right-hand side of Eq. (3) maintains the hyperbolic tangent phase-field profile across the diffuse interface, while cancelling out any curvature-driven interface motion. The reader is referred to [3, 8] for a detailed discussion of this technique.

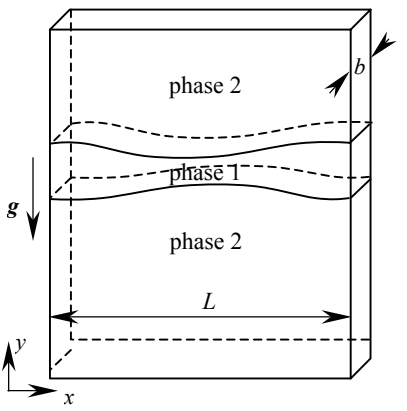

Figure 1: Schematic of the two-phase Hele-Shaw cell problem (after [2]).

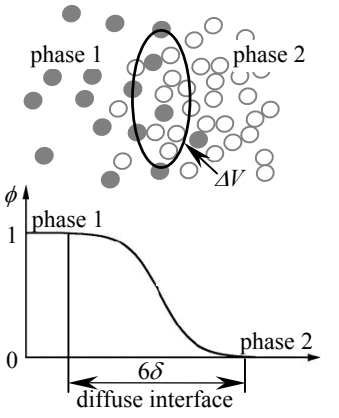

Figure 2: Schematic illustration of the diffuse interface and the phase field variation normal to the interface.

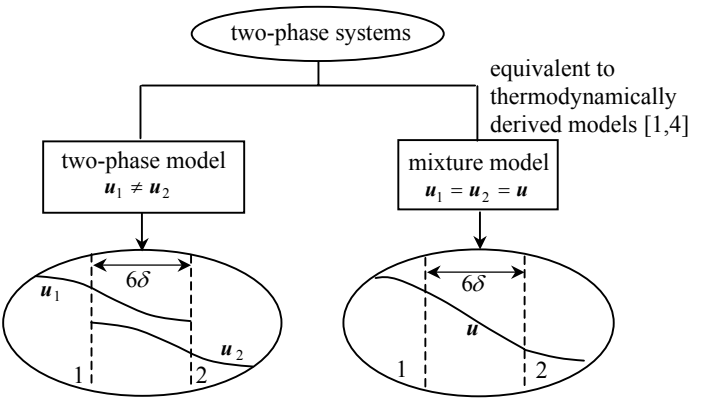

Figure 3: Illustration of the two-phase and mixture approaches.

2.1.2 Momentum

The momentum equations for the mixture velocity and the slip velocity are given, respectively, by

$$\boldsymbol{u} = -\frac{b^2}{12\mu} k_{rel}\left[\nabla p + \frac{\sigma\delta}{\phi(1-\phi)}\nabla^2\phi\nabla\phi - B\rho\boldsymbol{g}\right] \tag{4}$$

$$\Delta\boldsymbol{u} = -\frac{b^2}{12}\frac{\mu_2-\mu_1}{\mu_1\mu_2}\left[\nabla p + \frac{\sigma\delta}{\phi(1-\phi)}\nabla^2\phi\nabla\phi\right] + \frac{b^2}{12}\frac{\rho_1\mu_2-\rho_2\mu_1}{\mu_1\mu_2}\boldsymbol{g} \tag{5}$$

where $\mu = \mu_1\phi + \mu_2(1-\phi)$ is the mixture viscosity, μ_1 and μ_2 are the viscosities of phases 1 and 2, respectively, p is the mixture pressure, σ is the surface tension, and $\boldsymbol{g}$ is the gravitational acceleration. In Eq. (4), the relative "permeability", k_{rel}, is given by

$$k_{rel} = 1 + \frac{(\rho_2\mu_1 - \rho_1\mu_2)(\mu_1-\mu_2)}{\rho\mu_1\mu_2}\phi(1-\phi) \tag{6}$$

and the relative "kinetic" density, B, by

$$B = 1 + \frac{(\rho_2-\rho_1)\mu(\rho_2\mu_1-\rho_1\mu_2)\phi(1-\phi)}{\rho^2\mu_1\mu_2 + \rho(\rho_2\mu_1-\rho_1\mu_2)(\mu_1-\mu_2)\phi(1-\phi)} \tag{7}$$

These two factors are different from unity only inside the diffuse interface. Note that, $k_{rel}=1$ for $\mu_1=\mu_2$ and $B=1$ for $\rho_1=\rho_2$. The term $\sigma\delta\nabla^2\phi\nabla\phi/\phi(1-\phi)$ represents the surface tension force and is equivalent to the capillary stress term in thermodynamically derived models [1, 4] (see Ref. [6] for detail). Equation (5) shows that the slip velocity is non-zero only in the presence of property differences between the phases.

2.2 Mixture model

Setting $\Delta\boldsymbol{u}=0$, the mixture velocity, $\boldsymbol{u}$, becomes solenoidal (i.e., $\nabla\cdot\boldsymbol{u}=0$), and the last term on the left-hand side of Eq. (3) vanishes. The relative permeability, k_{rel}, and kinetic density, B, in Eq. (4) are both equal to unity.

3 Problem description and validation

The physical problem considered in the present study is adopted from [2]. As illustrated in Fig. 1, an unstable stratification is introduced by surrounding a layer of a light fluid, phase 1, by a heavy fluid, phase 2. The initial locations of the interfaces are given by $(x, y_1(x,0))$ and $(x, y_2(x,0))$, where [2]

$$\begin{cases} y_1(x,0) = \pi - (0.5 + 0.1\cos x) \\ y_2(x,0) = \pi + (0.5 + 0.1\cos x) \end{cases} \qquad 0 \le x \le 2\pi \tag{8}$$

Here, x and y are nondimensionalized by $L_0 = L/2\pi$. Periodic boundary conditions are applied in both the x and y directions. Under gravity, the upper interface is unstable and the upper heavy fluid flows downwards through the layer of light fluid. The lower interface is stable and resists motion. Ultimately, the two interfaces meet and pinch off. The equations are nondimensionalized using L_0, $t_0 = \mu_2 L/2\pi b^2(\rho_1 - \rho_2)g$, $u_0 = L_0/t_0$, and $p_0 = (\rho_1 - \rho_2)gL/2\pi$ as the length, time, velocity, and pressure scales, respectively. Two dimensionless parameters, the Bond number, $Bo = (\rho_1 - \rho_2)g(L/2\pi)^2/\sigma$, and the Atwood number, $At = (\mu_2 - \mu_1)/(\mu_2 + \mu_1)$, characterize the interface motion [2, 3]. Symbols denoting dimensionless variables are dropped in the following.

The numerical implementation of the present models (not described here due to space limitations) is validated by comparing results to the boundary-integral, sharp interface solution provided by Lee et al. [2]. The governing parameters for the validation case are [2]: density ratio $r_\rho = \rho_1/\rho_2 = 0.9$, viscosity ratio $r_\mu = \mu_1/\mu_2 = 1$, and $Bo = 25$. The mesh size is 250×250 grid points and $\delta = 0.04$. Calculated interface contours before pinch-off (at $t = 0$, 4, 6, and 7.5) are compared in Fig. 4. Note that a boundary-integral solution cannot be obtained during and after pinch-off [2]. It can be seen that the results from the present two-phase and mixture models almost overlap. This can be expected because in this example the viscosity ratio is equal to unity and the density ratio is also close to one. The diffuse interface results are in good agreement with the sharp interface solution, except near the pinch-off time (i.e., at $t = 7.5$). At that time, the diffuse interfaces are starting to overlap. Similar differences between diffuse and sharp interface results near the pinch-off have also been observed by Lee et al. [2]. They used a Cahn-Hilliard type (mixture) diffuse interface model with concentration as the order parameter.

The differences between the diffuse and sharp interface results before pinch-off can be attributed to the diffuse interface model results not being fully converged with respect to the interface width, δ. Identical results can only be expected for $\delta \to 0$. Figure 5 compares the convergence behaviour of the two-phase and mixture models with respect to δ. The calculated y intercept of the upper interface (i.e., the $\phi = 0.5$ contour), y_δ, at $t = 7.5$ is used as the figure of merit. The reference intercept, y_0, is obtained from the sharp interface solution of [2]. It can be seen that for a finite interface width, y_δ differs significantly from the sharp interface result. The two-phase and mixture models show both a

linear convergence behaviour with respect to δ. However, for a given interface width, more accurate results are obtained by the two-phase model, even though the density contrast is small and $r_\mu = 1.0$ in this case.

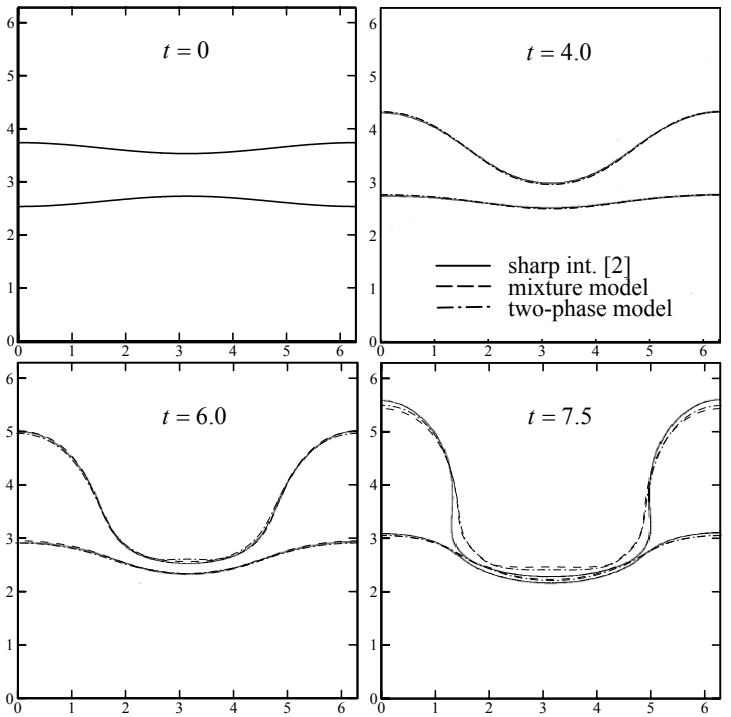

Figure 4: Evolution of interfaces: comparison between sharp and diffuse interface solutions ($r_\rho = 0.9$, $r_\mu = 1.0$, $Bo = 25$, and $\delta = 0.04$).

4 Results for large property contrasts between the phases

The two-phase and mixture models can be expected to differ more significantly for larger property contrasts between the two phases than in the previous test case. In the example of this section, the density and viscosity ratios are chosen to be $r_\rho = 0.01$ and $r_\mu = 0.1$. These ratios should be viewed as corresponding to a much less dense and less viscous phase 1 (middle fluid layer) compared to phase 2. The Bond number is kept unchanged by adjusting $\boldsymbol{g}$. The focus in the following discussion is on (i) the topology transition around the pinch-off time and (ii) the convergence of the results with respect to the interface width.

The calculated evolution of the phase-field contours for this example is shown in Fig. 6 for both the two-phase and mixture models. It can be seen that

the pinch-off occurs earlier for the two-phase model than for the mixture model. Also, at $t = 2.0$, two satellite drops appear for the two-phase model, while only a single but larger droplet occurs for the mixture model. The difference in the pinch-off time can be attributed to the presence of a highly asymmetric (with respect to $\phi = 0.5$) velocity distribution across the diffuse interface for the mixture model. For that model, the velocity inside the diffuse interface is dominated by phase 2, because that phase has a much larger density and viscosity. Since phase 2 is more viscous than phase 1, the velocity of phase 2 near the interface is generally less than that of phase 1. Hence, the asymmetric velocity distribution slows down the interface motion. The two-phase model effectively prevents this asymmetry because a slip flow is allowed inside the diffuse interface.

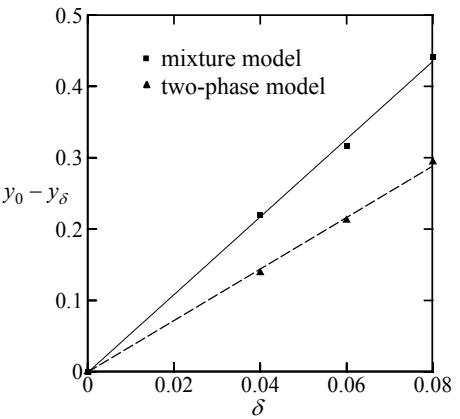

Figure 5: Convergence of y intercept of the upper interface at $t = 7.5$ wrt. δ ($r_\rho = 0.9$, $r_\mu = 1.0$, and $Bo = 25$).

The differences in the calculated velocities between the two-phase and mixture models can be better observed in Fig. 7. This figure compares results from the two models at different times, but in each case the results correspond to times right before and after the pinch-off. It can be seen that the velocities near the interface inside of phase 1 are generally smaller for the mixture model (Fig. 7a) and than for the two-phase model (Fig. 7b). This is particularly evident near the centre of the main vortex. Again, the smaller phase 1 velocities for the mixture model can be attributed to the more viscous and dense phase 2 extending its influence far across the diffuse interface into phase 1. The slip velocities inside the diffuse interface, $\phi(1-\phi)\Delta\boldsymbol{u}$, calculated by the two-phase model are shown in Fig. 7c. It is apparent that the velocity of phase 1 inside the diffuse interface is much larger than that of phase 2, which is due to the density and viscosity being smaller in phase 1 than in phase 2 [see also Eq. (5)]. Since $\boldsymbol{u} = \left[\rho_1\phi\boldsymbol{u}_1 + \rho_2(1-\phi)\boldsymbol{u}_2\right]/\rho$, the mixture velocity for the two-phase model is

therefore more symmetric across the interface, even though $\rho_1 << \rho_2$. Also note that it is the slip velocities shown in Fig. 7c that are responsible for the compressibility effect in the two-phase model, as discussed in connection with the continuity equation.

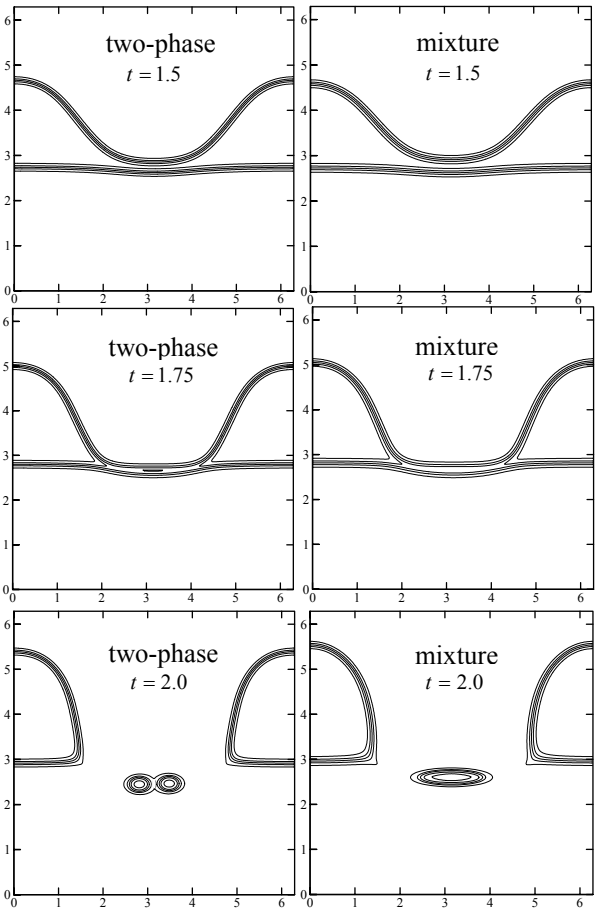

Figure 6: Evolution of phase-field contours ($\phi = 0.1$, 0.3, 0.5, 0.7, and 0.9) near the pinch-off: comparison of two-phase and mixture models ($r_\rho = 0.01$, $r_\mu = 0.1$, $Bo = 25$, $At = 0.82$, and $\delta = 0.04$).

A comparison of the convergence behaviour of the pinch-off time with respect to the interface width between the two-phase and mixture models is shown in Fig. 8. In each simulation, the grid spacing was adjusted such that $\Delta x/\delta = 0.628$, implying that the simulations with a smaller interface width required a finer grid. It can be seen that for both models, the pinch-off time

decreases in an approximately linear fashion with decreasing interface width. Best straight-line fits to the calculated results show that the pinch-off times from the two models converge to approximately the same value (~1.7) in the limit of $\delta \to 0$. As already noted in connection with Fig. 5, at a given interface width, the results from the two-phase model are much more accurate than those from the mixture model. For example, the pinch-off time for the mixture model with $\delta \approx 0.03$ is approximately the same as for the two-phase model with $\delta = 0.06$. Hence, the two-phase model offers a significant advantage relative to a standard mixture approach for large property contrasts between the phases. The remaining dependence of the two-phase model results on the interface width can be attributed to the presence of δ in the capillary stress term in the momentum equation.

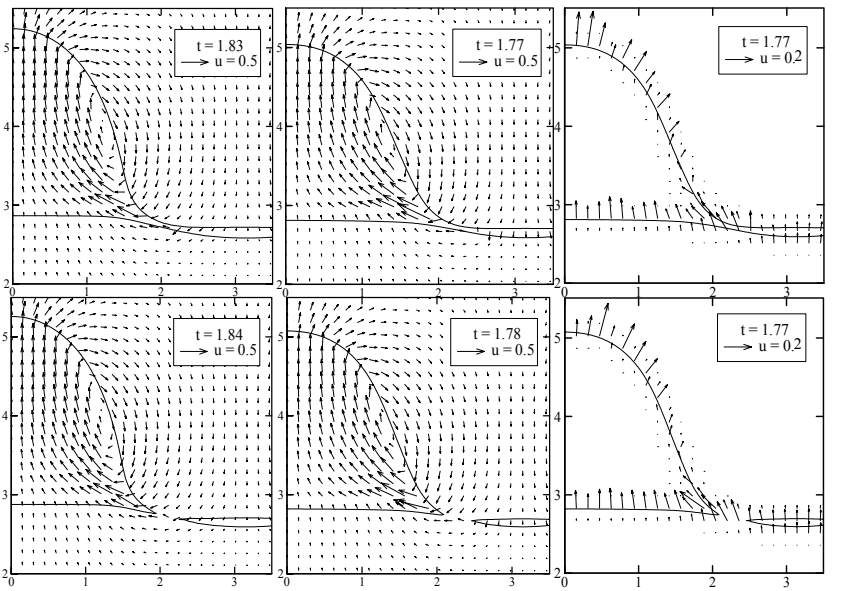

(a) $\boldsymbol{u}$: mixture (b) $\boldsymbol{u}$: two-phase (c) $\phi(1-\phi)\Delta\boldsymbol{u}$: two-phase

Figure 7: Velocity vectors before (upper panels) and after (lower panels) pinch-off ($r_\rho = 0.01$, $r_\mu = 0.1$, $Bo = 25$, $At = 0.82$, and $\delta = 0.04$).

5 Conclusions

The present study shows that, in the presence of large property contrasts between the phases, the use of a two-phase approach in diffuse interface modeling of micro-scale two-phase flows offers a significant advantage relative to standard models that assume a single velocity inside the diffuse interface. The two-phase

approach strongly reduces the dependence of the results on the width of the diffuse interface. Even though the present study examines only a simplified set of diffuse interface equations for Hele-Shaw flows, a similar advantage can be expected for the full Navier-Stokes version of the two-phase model as presented in [6]. Future work should focus on developing methods to overcome the remaining interface width dependencies due to the capillary stress term in the momentum equation. The ultimate goal of such work should be to achieve complete convergence of the results for a finite interface width (since only finite interface widths can be resolved numerically), along the same lines as in the thin-interface phase-field models of Karma and Rappel for solidification [10]. Only then can diffuse interface models be used reliably for the simulation of complex two-phase flows.

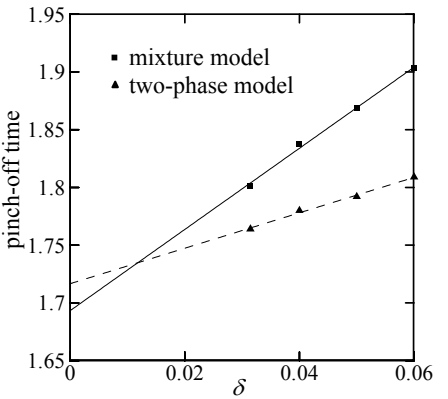

Figure 8: Convergence of pinch-off time wrt. δ ($r_\rho = 0.01$, $r_\mu = 0.1$, $Bo = 25$, and $At = 0.82$).

Acknowledgement

This work was supported by the U.S. National Science Foundation under Grant No. DMR-0132225.

References

[1] Jacqmin, D., Calculation of two-phase Navier-Stokes flows using phase-field modeling. *J. Comput. Phys.*, **155**, pp. 96-127, 1999.

[2] Lee, H.-G., Lowengrub, J.S. & Goodman, J., Modeling pinchoff and reconnection in a Hele-Shaw cell. I. The models and their calibration & II. Analysis and simulation in the nonlinear regime. *Phys. Fluids*, **14**, pp. 492-513 & pp. 514-545, 2002.

[3] Folch, R., Casademunt, J., Hernández-Machado, A. & Ramírez-Piscina, L., Phase-field model for Hele-Shaw flows with arbitrary viscosity contrast. I. Theoretical approach & II. Numerical study. *Phys. Rev. E*, **60**, pp. 1724-1733 & pp.1734-1740, 1999.

[4] Anderson, D.M., McFadden, G.B. & Wheeler, A.A., Diffuse-interface methods in fluid mechanics. *Ann. Rev. Fluid Mech*., **30**, pp. 139-165, 1998.

[5] Beckermann, C., Diepers, H.-J., Steinbach, I., Karma, A. & Tong, X., Modeling melt convection in phase-field simulations of solidification. *J. Comput. Phys*., **154**, pp. 468-496, 1999.

[6] Sun, Y. & Beckermann, C., Diffuse interface modeling of two-phase flows based on averaging: mass and momentum equations. *Physica D*, **198**, pp. 281-308, 2004.

[7] Anderson, D.M., McFadden, G.B. & Wheeler, A.A., Phase-field model of solidification with convection. *Physica D*, **135**, pp. 175-194, 2000.

[8] Sun, Y. & Beckermann, C., Interface tracking using the phase-field method (in preparation).

[9] Saffman, P.G. & Taylor, G., The penetration of fluid into a porous medium or Hele-Shaw cell containing a more viscous liquid. *Proc. R. Soc. London A*, **245**, pp. 312-329, 1958.

[10] Karma, A. & Rappel, W.-J., Phase-field model for computationally efficient modeling of solidification with arbitrary interface kinetics. *Phys. Rev. E*, **53**, pp. R3017-3020, 1996.